2021 EAGE ANNUAL
82ND CONFERENCE & EXHIBITION
AMSTERDAM | THE NETHERLANDS

FWI TO FULL BANDWIDTH WITH VECTOR REFLECTIVITY AND INVERSE SCATTERING IMAGING CONDITION, CLAIR FIELD OBN

Ø. Korsmo[1], T. Tshering[1], A. Pankov[1], P. Tillotson[2], D. Davies[2], L. Smith[2]

[1] PGS; [2] bp

Summary

Depth imaging in complex geology requires an accurate background model. In this case study, over the Clair field, we make use of high density node data set and Full Waveform Inversion (FWI) with Inverse Scattering Imaging Condition and Vector Reflectivity to solve the low wavenumbers in the model. The purpose of FWI was to capture the hard and fast seafloor followed by a strong velocity inversion, numerous localized high velocity bodies and accumulations of gas in the overburden, as well as mapping the rotated fault blocks in the target interval below Base Cretaceous Unconformity.

The inversion was done with a wavelet estimated from the data, to avoid possible bias in model updates related to phase errors in the deterministic wavelet. After solving the background model, the inversion continued up to 60 Hz. The final FWI model provided a well focused image with realistic structures and a flatter gas-oil contact than the vintage model. Significant amount of details have been captured in the FWI model, which correlates well to sonic data and the geological knowledge of the area.

FWI to full bandwidth with Vector Reflectivity and Inverse scattering Imaging Condition, Clair field OBN

Introduction

Depth imaging in complex geology requires an accurate background model. Recent developments in Full Waveform Inversion (FWI) have simplified and automated this process through a new implementation of the wave equation combined with a unique imaging condition that separates the tomography and the impedance kernel in FWI. We demonstrate this on an Ocean Bottom Node (OBN) data set, covering the Clair field in the UK sector.

The Clair field is located 70 km West of Shetland, and is UK's largest naturally fractured reservoir. The overburden is highly complex, this includes an old hard seafloor followed by a strong velocity inversion, a series of high velocity geobodies, believed to be cemented sands, and several pockets of gas. In 2017, a new ultra high density OBN survey was acquired to improve the imaging (Tillotson et al., 2019). The reservoir is located between 1500 and 2500 meters depth, in the rotated fault blocks below the Base Cretaceous Unconformity (BCU). The aim of FWI was to capture all these complexities and provide an accurate imaging model.

Estimation of source wavelet

In FWI, the source wavelet is forward propagated through the initial velocity model and compared to the observed data. Phase misalignments between the two data sets (data residuals) are back propagated to form the gradient that updates the model in the least-squares inversion. Errors in the source wavelet can lead to incorrect model updates and a badly conditioned inversion. Thus, we start by estimating the source wavelet in the frequency domain by solving a linear inverse problem (e.g., Vireux and Operto, 2009). This inversion is done for the direct arrivals on a shot by shot basis, and the average wavelet becomes the new FWI source. The hard boundary conditions will add ghosts and multiples consistent with the observed response. Figure 1a-b-c shows the initial and inverted wavelet together with the spectra comparison. The observed and modeled response are shown in figure 1d-e-f. The raw observed data (figure 1d) shows a mixed phased response from the source wavelet and instrument filter, while the initial wavelet and modeling (figure 1a, e) is perfectly zero phased. The inverted wavelet (figure 1b) is asymmetric, and combines the actual source wavelet and the instrument response. The new modeling (figure 1f) compares better to the observed data than the initial wavelet, which is most evident around the direct arrival (white arrow) and the water bottom peg-leg.

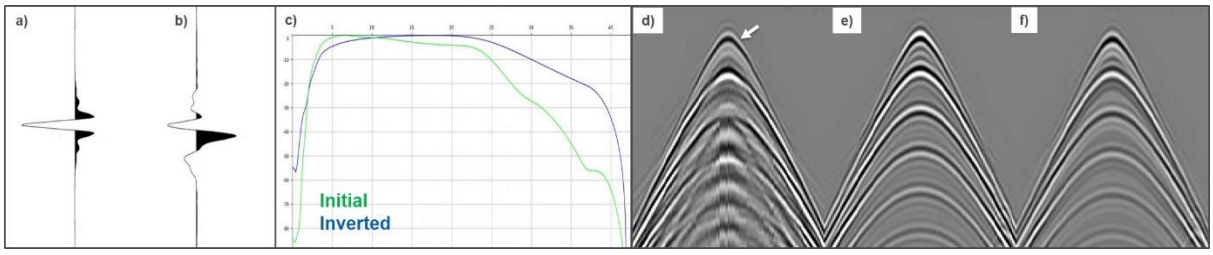

Figure 1: Initial (a) and estimated (b) wavelet. Comparison of the amplitude spectrums (c). Observed data (d), modeled data with initial wavelet (e) and the inverted wavelet (f).

Inverse Scattering Imaging Condition and Vector Reflectivity

FWI and Reverse Time Migration (RTM) use the same wavefield modeling engine and hence share the same kernel. Figure 2a shows the kernel for a single source-receiver location using crosscorrelation imaging condition. The velocity model generate a diving wave (1), from the linear increase in velocity, and low frequency transmitted (2) and high frequency scattered energy (3) from the sharp velocity boundary. The migration isochrone (3) can be several orders higher in magnitude compared to the low frequency transmitted energy from the reflector (2), also referred to as the velocity kernel. Ramos-

Martinez et al. (2016) proposed a FWI implementation with Inverse Scattering Imaging Condition (ISIC) that separates and suppress the migration isochrones from the velocity kernel as illustrated in figure 2b. This enable us to accurately solve the crucial low wavenumbers in the model that matters for imaging, using the entire wavefield, meaning beyond the penetration depth of diving waves.

Reflection-inclusive FWI requires hard boundaries in either the density or velocity model. This may be difficult, when an accurate density model is not available, or the velocity model is immature or inaccurate. Our FWI method use an alternative approach based on Vector Reflectivity in the wave-equation to initiate reflections during forward modeling (Yang et al., 2020). We provide FWI with an image of the seismic reflectivity which then generates the observed reflections and enables us to update the background model with ISIC. Figure 2c shows the observed and modeled data with Vector Reflectivity. One can see that the observed events (reflections and diving waves) are produced by the forward modeling and compares well with the observed data. The FWI with ISIC will update the model and change the kinematics of these events in the data domain.

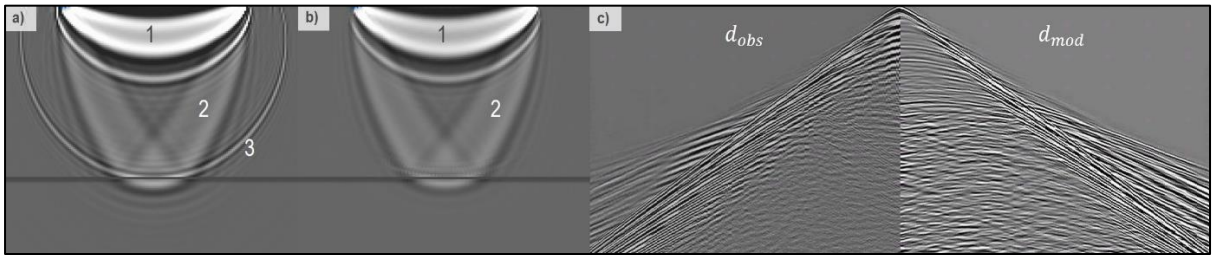

Figure 2: FWI sensitivity kernel using Crosscorrelation Imaging Conditon (a) and Inverse Scattering Imaging Conditon b). The diving energy is annotated as (1), low frequency transmitted energy (2) and the migration isochrone (3). The Inverse Scattering Imaging Conditon suppress the migration isochrone and enables FWI to solve the background model. Figure (c) shows the observed and modeled data using Vector Reflectivity.

FWI and imaging results

The FWI process started with a smooth version of the vintage model and followed a classical multi-scale approach; starting from low to high frequencies and gradually growing the data selection based on the match between the observed and modeled response until most of the data was utilized in the inversion. The first iterations were done with a maximum frequency of 4 Hz. After solving the crucial low wavenumbers in the model, the inversion continued up to 60Hz to provide further details about the lithology and the structural extension of local velocity variations in the overburden. The model was updated from top to bottom, controlled by the data selection. We first utilized the early arrivals and grow the selection to full offset range before we targeted the near to mid offsets reflections.

Figure 3a-b shows the vintage and the new FWI model for an arbitrary line through two wells in the area with the image overlaid. The vintage model captured the main structures below BCU, but it did not represent the complicated overburden correctly when comparing it to the sonic profile at Well B, as annotated by the two white arrows. Comparing this depth interval in the vintage and new FWI model, shows that the FWI process has re-allocated the fast velocities shallower and removed the fast (green) layer annotated by the second white arrow on the vintage model. These corrections can be confirmed with the well data in figure 3c, where the same features have been annotated in the sonic profiles as for the velocity displays. Details in the FWI model seem structurally consistent with the image as well as providing a good correlation to the sonic trends. The red arrow, at Well B (figure 3c), shows sonic velocities up to 5000 m/s. The FWI did not capture these high velocities, but there are several reasons that could account for the observations. The velocity variations could be incorrect, related to bad coupling or casing issues, or it could be that these high values are limited to a very local anomaly. The structural imaging and evaluation of gather flatness at the well location, did not suggest that these extreme velocities should be part of the imaging model.

Figure 4 shows the imaging response for the vintage a) and the new FWI model b) with a Kirchhoff PSDM migration. The arrows points at the gas-oil contact (GOC) with seismic black polarity. The FWI model resolved most of the overburden effects and consequently simplified the structural image, which flattened the GOC compared to the vintage migration. The lateral consistency of the FWI model can be seen in the depth slices in figure 5.

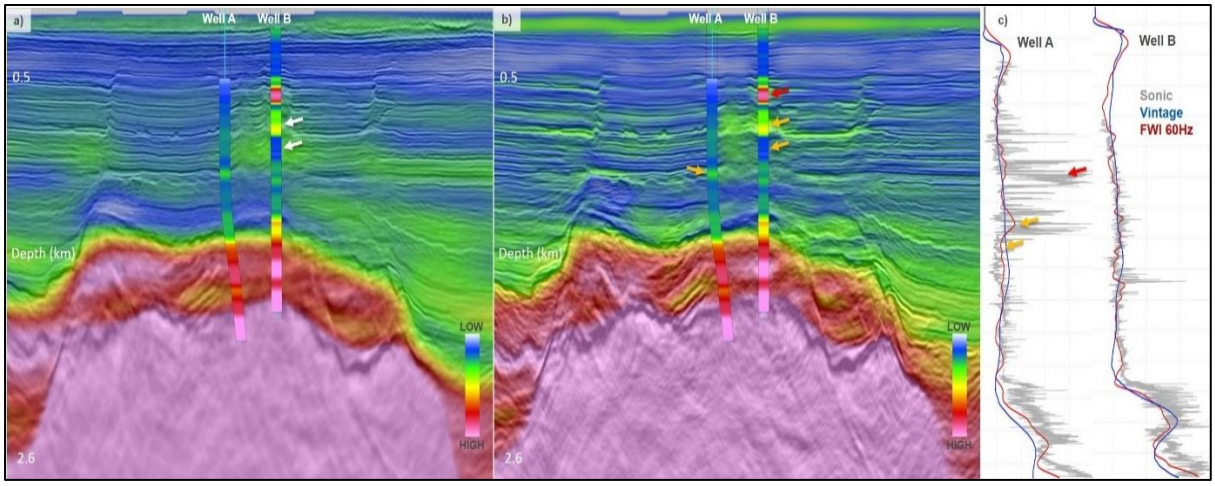

Figure 3: Vintage model overlaid on the vintage image (a) and the new FWI model and updated image (b). Sonic log (gray) compared to the vintage (blue) and the new FWI model (red) for two wells (c). Notice the structural consitency and match to the sonic profile achieved with the new FWI model. The white and orange arrows indicate areas where the FWI model have redistributed the local velocity variations in the overburden and provided a model that better agrees with the sonic profile. The red arrow shows an interval with extreme high values. This has not been picked up by the FWI process but it is not supported by the imaging response.

Conclusions

In this case study, we have demonstrated the ability to build an accurate background model for imaging based on our unique implementation of FWI using the high density OBN data over the Clair field. The separation and suppression of the migration isochrones combined with Vector Reflectivity built an accurate background model with both diving waves and reflection data. After solving the background trend, the inversion continued up to 60 Hz to provide structural information of the local velocity variations in the overburden. To reduce potential errors with the wavelet, we inverted for the source wavelet prior to the FWI process. The overall image uplift from the new FWI model resulted in a more realistic seismic structures, a flatter GOC and good correlation to the sonic trends.

Acknowledgements

The authors wish to thank bp and the Clair JV partnership for permission to show the results. Furthermore we thank Yang Yang, Jaime Ramos-Martinez, Norman Daniel Whitmore, Bertrand Caselitz, Tony Martin, and Julien Oukili at PGS for their valuable support.

References

Ramos-Martinez, J., S. Crawley, K. Zou, A. A. Valenciano, L. Qiu and N. Chemingui [2016] A robust gradient for long wavelength FWI updates, 78th EAGE Conference & Exhibition, Extended Abstracts.
Tillotson, P., Davies, D., Ball, M and Smith, L [2019] Clair Ridge: Learnings From Processing the Densest OBN Survey in the UKCS, 81th EAGE Conference & Exhibition, Extended Abstracts.
Virieux, J., and Operto, S. [1999] An overview of full-waveform inversion in exploration geophysics. Geophysics, **74**, 6, WCC1-WCC26.

Yang, Y., J. Ramos-Martinez, N. D. Whitmore, A. A. Valenciano, G. Huang and N. Chemingui [2020] FWI using reflections for deep velocity model updates, 90th SEG Annual International Meeting, Expanded Abstracts, 691-695.

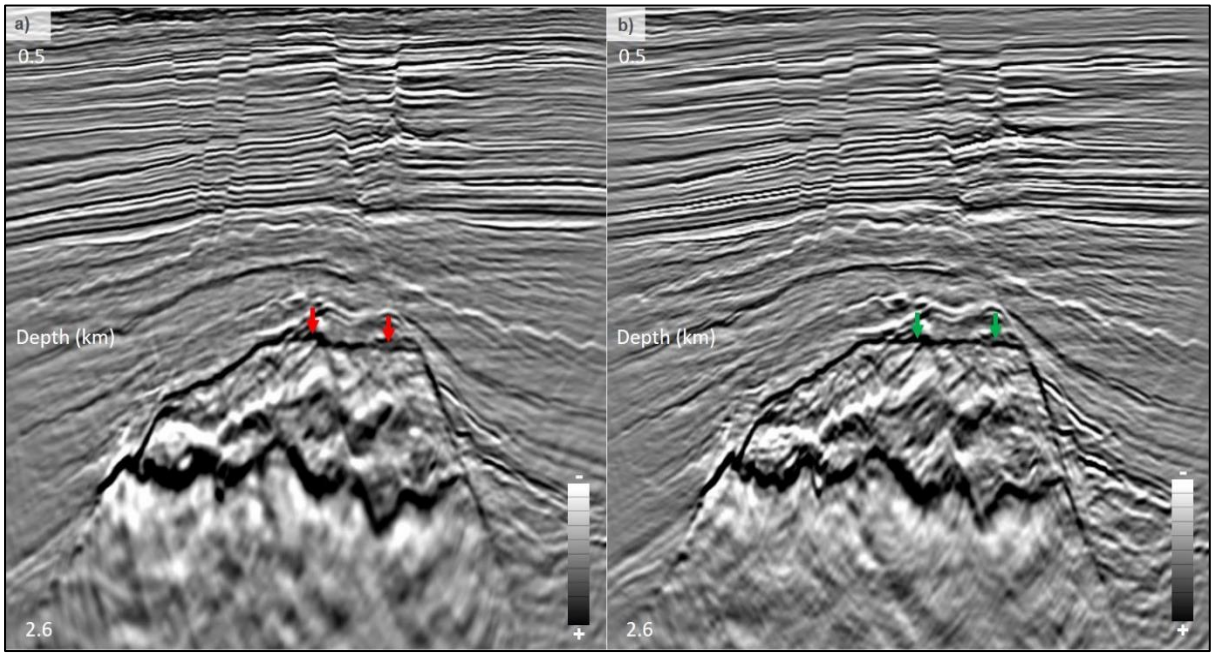

Figure 4: Imaging with the vintage model (a) and the final FWI model (b). The new FWI model changes the structural image and provides a more realistic and flat GOC (red and green arrows) compared to the vintage model results.

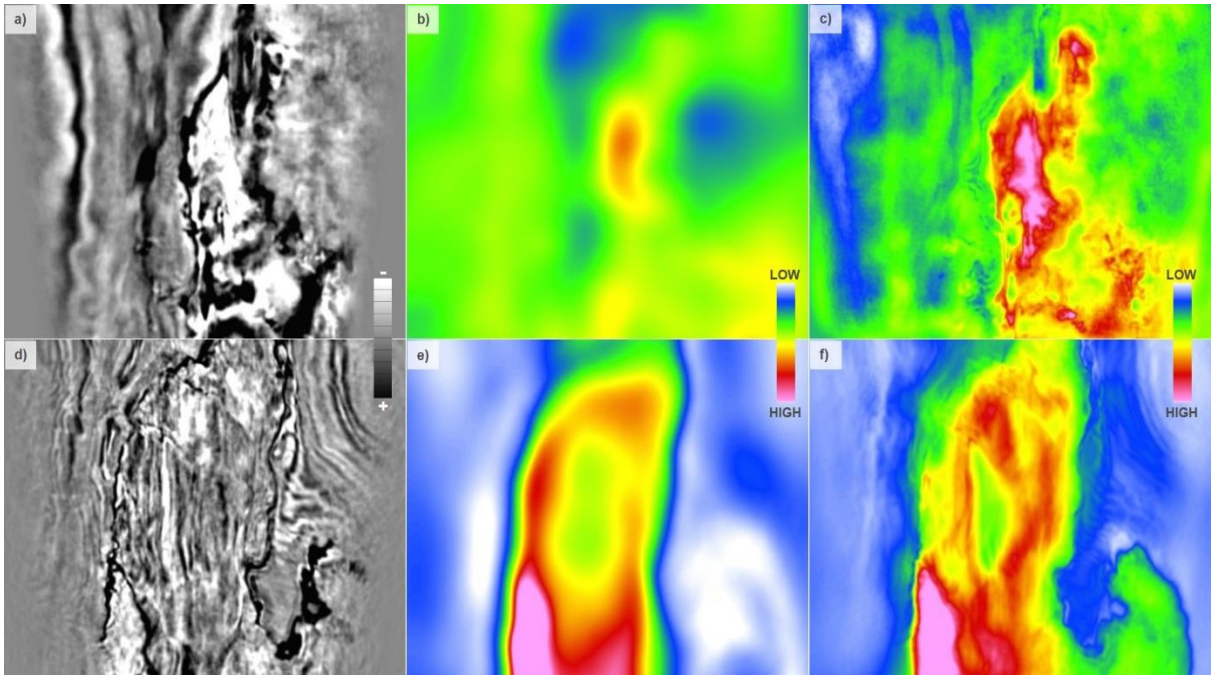

Figure 5: Depth slice at 0.8 km (a). The final migration with the final FWI model. (b) The vintage velocity model (c). The final FWI model. The same illustration at depth slice 1.7 km (d, e, f). Notice the structural consitency and details achieved with the new FWI model.